

Drag on Bluff Bodies

Felicity Cundiff, Angelina dos Remedios, Peter Funston, Kyle Klem
AA 321 Aerospace Laboratory, Section Code
William E. Boeing Department of Aeronautics, University of Washington
2023-01-24

I. Nomenclature

p_{front}	=	Pressure on the front surface
p_{back}	=	Pressure on the back surface
ρ	=	Density
V	=	Velocity
L	=	Length
μ	=	Viscosity
F_d	=	Drag Force
A	=	Reference Area

$$C_D = \frac{F_d}{\frac{1}{2}\rho v^2 A} \quad (1)$$

$$Re = \frac{\rho v L}{\mu} \quad (2)$$

$$C_p = \frac{p_{front} - p_{back}}{\frac{1}{2}\rho V^2} \quad (3)$$

$$\text{percent error} = \frac{|\text{experimental value} - \text{theoretical value}|}{\text{theoretical value}} \times 100 \quad (4)$$

II. Results/Discussion

The main objective for this laboratory experiment is to investigate drag on a bluff body. As well as how it varies with the Reynolds number found, which is a measurement of the flow characteristics of a fluid surface over a surface involved. This is done by conducting a series of tests utilizing the 3' x 3' wind tunnel. The sequence of testing began with the balance fairing for tare, followed by the 5 inch disk, the 5 inch sphere, the large trip ring, and finally the smaller trip ring. Before the experiment took place, using the University of Washington Department of Atmospheric Sciences the atmospheric pressure in Seattle, Washington was recorded to be 14.90Psi at 1:30 pm. As the velocity consistently increased during testing with the objects inside the wind tunnel, the temperature recorded stayed between 13 degree Celsius and 16 degrees Celsius.

Now for each body being tested, the velocity inside the tunnel was increased a little bit at a time to achieve a quasi-steady state at each velocity until a dynamic pressure of about 25 psf was reached. Figure 1 shows this pattern of plateauing velocities. This it clearly seen in the disks test run. Originally a dynamic pressure of 45 psf was the desired dynamic pressure, however, due to safety concerns facility personnel reduced limit to 25 psf during the experiment. Over all, as the velocity increased at a slow rate so did the dynamic pressure until it reached the desired dynamic pressure. Also the program provided at the wind tunnel to measure the desired dynamics pressure at 25 psf, at differential pressure between the front and back of the test article (psf), and drag variable needed is LaBVIEW.

The variation of the drag coefficient and the Reynolds number for each of the test articles in the experiment greatly depend on the shape of it individually. Generally as the as the drag coefficient decreases the Reynolds number will

increase. As seen in figure 2, this is true for the disk, sphere, small and large trip ring test articles. To reiterate and draw a conclusion to the data, it is displayed very clearly showing a decay in the drag coefficient and an increase in the Reynolds number. These results can be compared to the publication "Drag of a Sphere" because in the real world this can apply to objects like a sports ball such as a soccer ball or a golf ball which has many dimples to reduce drag. Now referring to the Drag of Sphere test article, the Reynolds number is right before 10^5 and now with that in mind according to it, it is entering a turbulent flow. All of the test subjects start from a laminar flow and as the Reynolds number goes up, it starts laminar and steady all the way to a turbulent flow including their individual drag bucket.

In the results, the drag bucket will come from when the Reynolds number becomes constant while it makes a sharp dip in the drag coefficient value. This will be different for each of the test articles as shown in figure 2. The most noticeable test article that had the most dramatic drag bucket dip was the sphere with the small trip ring. The small trip ring test article displays the drag bucket happening at around a Reynolds number of $10^{4.8}$. It was a very big dip so much so that it was the lowest dip on the graph. The second most noticeable drag bucket turned out to be the sphere alone. The dip in the drag coefficient value was around the same Reynolds number again, which was $10^{4.8}$, but it also created a dip at the end of the test which was around a Reynolds number of $10^{5.7}$. The third test which was the sphere with the larger trip ring, it displayed a compact set of points reaching up and down in the beginning/middle of the run and after which it settled out linearly. Now lastly the fourth and final test article being the disk. It really did not display a drag dip at least in the data that was collected. It makes a steady decline down the graph. With this in mind the changes found in the drag coefficient were consistently declining as the Reynolds number increased like the previous test articles. Now the data that was collected in the lab experiment very closely follows the same C_d vs. Re graph presented in the "Drag of a Sphere" article.

Using equation 3, the pressure difference coefficient between the front and the back of the test article is calculated as a ratio of the pressure difference. The relationship between the pressure difference coefficient and the Reynolds number can help us understand the behavior of the flow. This will vary for each of the test articles. The pressure difference (C_p) can also be thought about as the pressure distribution over the surface of the disk for example. As seen in figures 2 and 3, the beginning of all of the tests that were conducted the flow appears to be laminar given the low Reynolds number and linear appearance, but as the velocity increases, the center of pressure moves closer to the center of the object at an exponential rate.

Fig. 1 Incremental Velocity Changes Throughout Tests

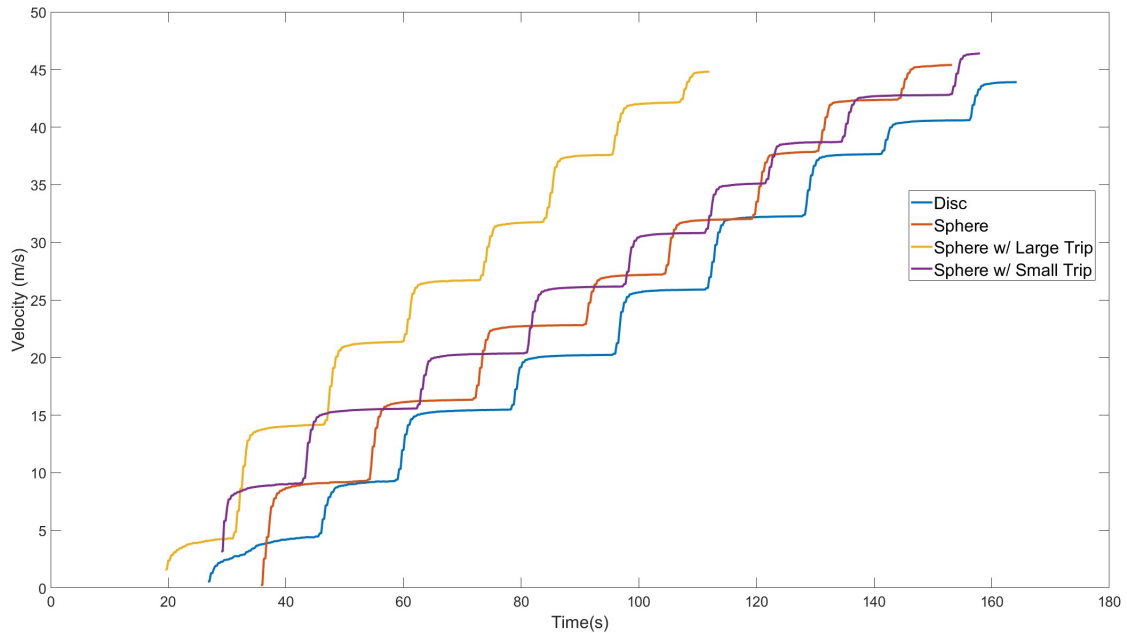
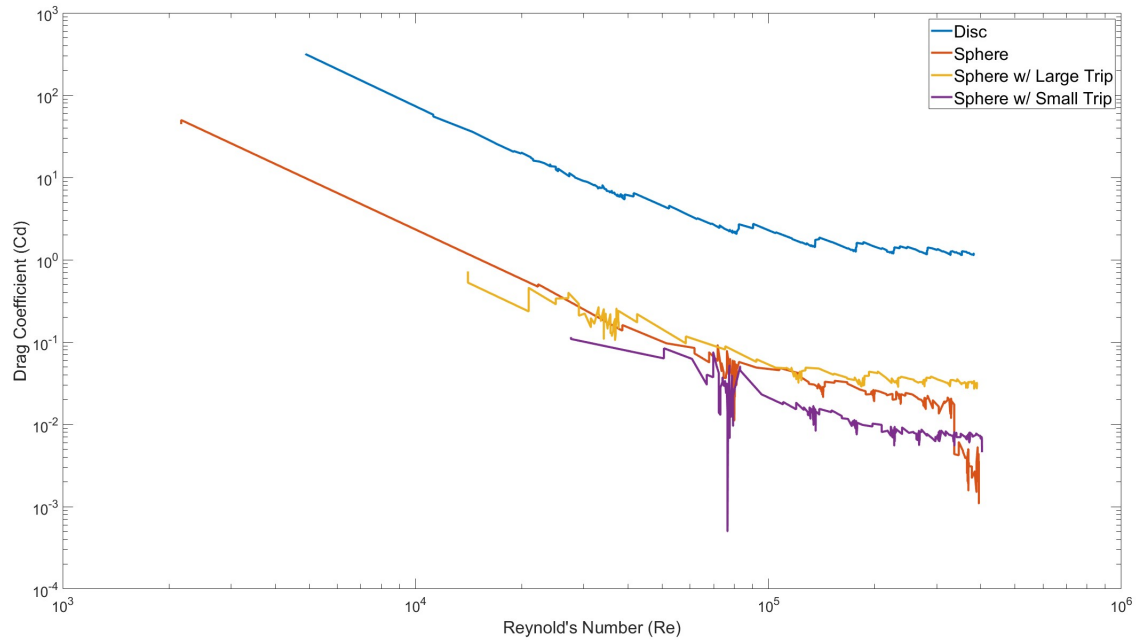


Fig. 2 Effects on Drag Coefficient and Reynold's Number as Geometry and Velocity Change

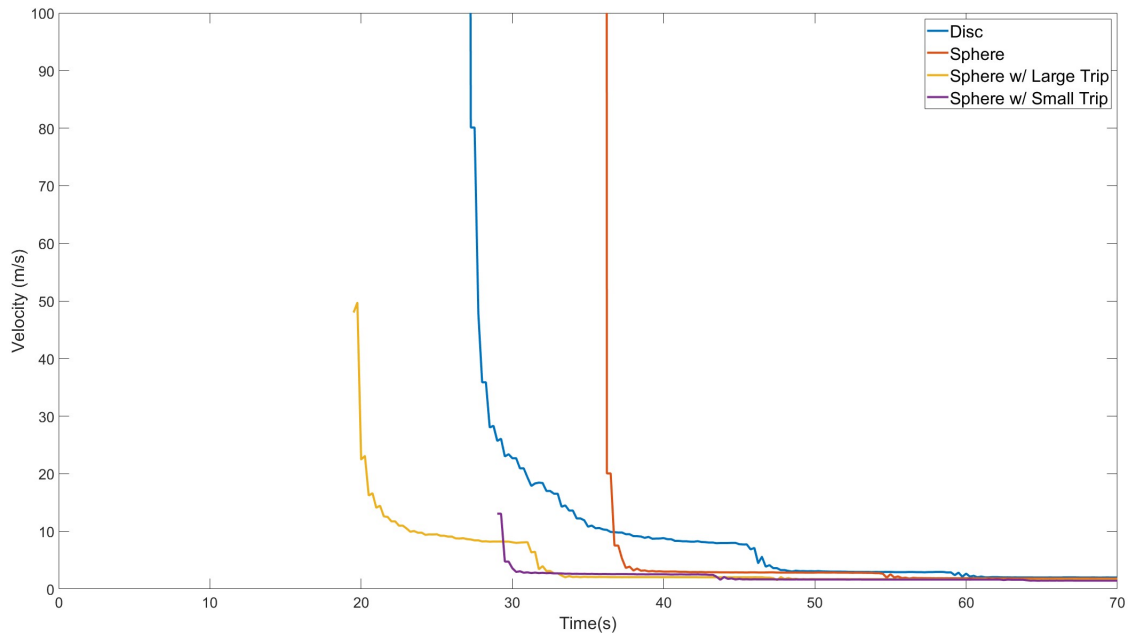


Examining the results for the three sphere tests there is a clear effect in each case. Comparing the lines in Figure 2 the sphere with no trip can be used as a base line to compare the other results. This line steadily decreases until a Reynold's number of $10^{4.8}$ where there is a drag bucket before continuing to steadily decline until a Reynold's number of $10^{5.7}$ where there is another drag crisis. Comparing this to the sphere with a small trip wire shows a line which looks quite similar. The noticeable differences are that the sphere with a small trip wire has less drag most of the time, the drag bucket at a Reynold's number of $10^{4.8}$ drops much farther, and there is no drag crisis when the Reynold's number is $10^{5.7}$. However, there is a dip right at the end of the data suggesting that there could be a drag crisis at a higher Reynold's value, had the test reached higher velocities. The line for a sphere with a large trip wire has a similar start to the other two lines, however, rather than having a drag bucket at a Reynold's number of $10^{4.8}$ it has one much earlier at $10^{4.4}$. Before the drag bucket, the line shows that the drag coefficient is a little bit lower to about the same as the sphere with no trip wire, but after the drag bucket the line remains almost always above the line for just a sphere showing it has a higher drag coefficient.

This experiment can help inform sports ball designs due to where drag buckets occur and the drag coefficient. Drag has an obvious effect on design since it directly effects the velocity of the object as well as the forces required to achieve that velocity. A great example of this is golf balls where you could design balls to have reduced drag in order to have them go farther. Drag buckets are also a useful part of design since it is a range of Reynold's numbers where you would get the least drag for that velocity. This is useful since for things like golf balls can be made such that their most common velocity lies within a drag bucket.

Looking at the errors throughout the experiment there are errors from the instruments used in the experiment the force measurements have an error of $\pm 0.25\%$, the ΔP has an error of $\pm 0.5\%$, and the temperature has an error of $\pm 1^\circ\text{C}$. These are the errors which will propagate through the results. There will also be a small amount of error from the measurements of length as well as the atmospheric pressure used in calculations. While the length and pressure errors do not have a large effect on the overall outcome, they do need to be considered as sources of error. Using the error from the aforementioned sources once propagated shows the errors for air density as $\pm 0.35\%$, velocity as $\pm 0.425\%$, Reynold's number as $\pm 0.775\%$, and drag coefficient as $\pm 1.45\%$. These error values are small enough that even with the unknown error from length and atmospheric pressure measurements, the data and conclusions from this experiment are still accurate.

Fig. 3 Effects on Center of Pressure as Geometry and Velocity Change



III. Conclusion

This experiment aimed to determine what effect, if any, Reynold's number, tripping devices, and the type of flow had on the body drag of a bluff body. This experiment took place in the UW 3' x 3' wind tunnel. Measurements were taken for five different objects: the balancing fairing, the disk, the sphere, and the sphere with two different-sized trips. The experiment started with a sensor tare, using the balancing fairing to correct the interference from the object mounts. The drag, indicated dynamic pressure of the tunnel, and the differential pressure between the front and back of the test article were displayed and measured by the LabVIEW program. One by one, each object was placed in the wind tunnel. The flow speed was increased until the induced pressure reached the maximum value of 25 psf, and the flow speed was decreased back to zero. This rendered data detailing how the induced pressure, the temperature, and the axial force changed with time for each object. Using this data, the graphs for drag coefficient vs Reynold's number were constructed and analyzed. As seen in figure 2, the drag on the disk was greatest, the drag on the sphere with the large trip was primarily more than that of the sphere with out trips or the sphere with the small trip. The drag coefficient for the sphere with the small trip was the smallest. Most interestingly, the drag coefficient for the sphere without trip shows a drag crisis at the high end of Reynold's numbers. It is presumed that the other three objects would display similar behavior if the wind tunnel could be faster. One limitation to this experiment was the rate at which the velocity was increased was not constant. For better data in future experiments, it would be wise to utilize LabVIEW to display the change in velocity, and strive for a consistent and repeatable increase in velocity.

References

Department of Atmospheric Sciences, 2023, <https://atmos.uw.edu/current-weather/>.

NASA. "Drag of a Sphere - Glenn Research Center." NASA, NASA, 24 June 2022, <https://www1.grc.nasa.gov/beginners-guide-to-aeronautics/drag-of-a-sphere/>.